THE IMPACT OF LAND-COVER CHANGE ON CARBON AND WATER CYCLING IN THE U.S. CENTRAL PLAINS GRASSLANDS

BY

Tyler Buck

Submitted to the graduate degree program in Geography and the Graduate Faculty of the University of Kansas in partial fulfillment of the requirements for the degree of Master of Science

---

Nathaniel Brunsell
Chairperson

David Mechem

Daniel Hirmas

Date Defended: June 25, 2010

The Thesis Committee for Tyler Buck
certifies that this is the approved version of the following thesis:

THE IMPACT OF LAND-COVER CHANGE ON CARBON AND

WATER CYCLING IN THE U.S. CENTRAL PLAINS GRASSLANDS

Nathaniel Brunsell
Chairperson

Date Approved: June 25, 2010

ACKNOWLEDGMENTS

This work was supported under the National Science Foundation EPSCoR program (NSF EPS 0553722) as well as KAN0061396/KAN0066263. Data for KZU and K4B prescribed fire burns was supported by the NSF Long Term Ecological Research Program at Konza Prairie Biological Station. The author would like to thank Dr. Nate Brunsell, Dr. Jay Ham, Kira Arnold, Fred Caldwell, Patrick O'Neal and Galen Pittman for their contributions.

Contents

List of Figures

List of Tables

Chapter 1

Introduction

Humans have had a profound impact on the Earth's surface. Anthropogenic land cover change has influenced the Earth's climate by altering ecosystems and the fluxes of mass and energy associated with them (Dale, 1997). A large portion of the Earth's terrestrial surface is covered by grasslands and over 70% of the world's agriculture is produced in these ecosystems (FAO, 2009). Therefore, it is imperative to study the possible impacts of land cover, land use and climate change on grassland ecosystems.

In order to assess the impact of climate and land cover change on grasslands ecosystems, a tool is needed to measure the exchange of energy and mass between the Earth's surface and the atmosphere. Currently, one of the best methods available is the eddy covariance technique, which allows direct measurement of turbulent fluxes of mass and energy exchange between the Earth's surface and atmosphere (Baldocchi et al., 2001a). Systems using this methodology are used in many different ecosystems all over the world. Many of the eddy covariance towers are part of regional research networks across the globe, including Ameriflux, CarboEuroFlux, AsiaFlux, and OzFlux (Aubinet et al., 2000; Baldocchi et al., 2001a). Due to its wide use in many different ecosystems, including grasslands, the eddy covariance technique is an

ideal methodology for studying the impacts of land-cover and climate change.

When using the eddy-covariance technique, it is vital to understand the underlying theory to interpret results as well as the assumptions and issues that are implicated. Resources such as Stull (1988) provide an overview of the governing theory underlying the eddy covariance technique. Turbulent fluxes measured by theses systems are sometimes underestimated, and therefore need to be corrected. Corrections such as frequency sampling, coordinate rotation, and lag removal are outlined in resources such as Lee et al. (2004), Massman (2000), Webb et al. (1980), and Paw U et al. (2000). However, there are issues with this system, with fluxes sampled by eddy covariance systems that do not conserve energy, the so-called energy balance closure problem (Twine et al., 2000; Wilson et al., 2002)

To examine how ecosystems respond to land cover and climate change, we can explore how efficiently plants assimilate carbon per-unit of water. This relationship is called "water-use efficiency". Although there are many ways to calculate water-use efficiency, a common method is determining the regression slope between assimilation and ecosystem evapotranspiration (Baldocchi et al., 2001a). Water-use efficiency can give insight into how ecosystems respond to land cover and climate change by assessing how the efficiency of carbon assimilation changes with vegetation composition.

The scientific problem that drives this study is how land-cover change impacts water and carbon cycling in grasslands in the central U.S. plains. To address this problem, the following objectives will be completed: 1) An overview of the eddy covariance technique, including the underlying theory, data processing procedures, and issues, and 2) analysis of how land cover impacts water-use efficiency in grassland ecosystems using eddy covariance methods. It is the overall goal of this study to help provide a better understanding of how grasslands in the central plains will respond land-cover change.

Chapter 2

Processing procedures for eddy covariance measurements

2.1 Introduction

Eddy covariance is a useful technique that allows measurement of the turbulent fluxes of mass and energy exchange between the Earth's surface and atmosphere. Measurement from these systems are used all over the world in different ecosystems (Baldocchi et al., 2001b). Generally, these measurements are taken at high frequencies (10-20Hz) to ensure that the high-frequency contributions to the flux are sampled adequately (Anderson et al., 1984; Baldocchi et al., 2001b). Although the eddy covariance methodology has been useful in measuring these turbulent fluxes, it also has its limitations. The methodology has issues with accurately closing the energy balance, sometimes on the order of 30% underestimation (Twine et al., 2000). These errors have been attributed to several factors ranging from random instrumentation error (Goulden, 1996) to spatial heterogeneity (Foken et al., 2009; Huang et al., 2009). Understanding how to properly process flux measurements and address these uncer-

tainties is important for long-term studies of water, carbon, and energy exchanges within an ecosystem (Massman and Lee, 2002).

As stated in Vickers and Mahrt (1997), there are three common errors associated with flux sampling:

1) Systematic errors due to the instrument's inability to detect all large-scale transport of fluxes. This would lead to an underestimation of the flux.

2) Random errors due to inadequate sampling of turbulent eddies.

3) Non-stationarity, or inhomogeneity of the the turbulent flow, which can lead to a dependence on the decision of an averaging scale.

To help reduce these errors and avoid uncertainties within the data, several processing and quality control procedures are conducted on high-frequency eddy covariance data. The focus of this chapter is to provide an overview of the eddy covariance technique and the specific procedures to insure proper determination of the turbulent fluxes.

2.2 Background Theory

In order to discuss the theory behind the eddy covariance technique, the governing equations that apply to the boundary layer are examined. Due to the complexity of atmospheric motions and the equations that are associated with them, we use approximations that average turbulent motions over smaller scales. The governing equations of boundary layer atmospheric motion are outlined in Stull (1988). Stull (1988) presents Newton's second law of motion, the conservation of momentum. Writ-

ing in standard tensor notation, the momentum equation can be expressed as:

$$\underset{\text{(I)}}{\frac{\partial U_i}{\partial t}} + \underset{\text{(II)}}{U_j \frac{\partial U_i}{\partial x_j}} = \underset{\text{(III)}}{-\delta_{i3} g} \underset{\text{(IV)}}{- 2\epsilon_{ijk}\Omega_j U_k} \underset{\text{(V)}}{- \frac{1}{\rho}\frac{\partial p}{\partial x_i}} \underset{\text{(VI)}}{+ \frac{1}{\rho}\frac{\partial \tau_{ij}}{\partial x_j}} \tag{2.1}$$

where Term I represents inertia, Term II describes advection, Term III is gravity (g), Term IV describes the Coriolis effect, Term V describes the pressure (p) gradient force, and Term VI represents the influence of viscous stress (Stull, 1988).

Expanding equation (2.1) and applying the Boussinesq approximation and Reynolds averaging, the coordinate system is aligned with the mean wind, while subsidence is neglected, and horizontal homogeneity is assumed. Coriolis effects, pressure diffusion, and molecular diffusion of turbulent flux are neglected due to their small scale and magnitude. Thus, the covariance of horizontal (u) and vertical (w) velocities ($\overline{u'w'}$), or the prognostic equation of turbulent flux for momentum is written as:

$$\underset{\text{(I)}}{\frac{\partial(\overline{u'w'})}{\partial t}} = \underset{\text{(II)}}{-\frac{\overline{w'^2}\partial\overline{U}}{\partial z}} \underset{\text{(III)}}{- \frac{\partial\overline{u'w'w'}}{\partial z}} \underset{\text{(IV)}}{+ \frac{g\overline{u'\theta'_v}}{\bar{\theta}_v}} \underset{\text{(V)}}{+ \overline{\frac{p'}{\overline{\rho}}\left(\frac{\partial u'}{\partial z} + \frac{\partial w'}{\partial x}\right)}} \underset{\text{(VI)}}{- 2\epsilon_{uw}} \tag{2.2}$$

where Term I describes the storage of the momentum flux, Term II describes the production of momentum flux due to wind shear, Term III describes the turbulent transport, Term IV describes the buoyancy, Term V is the pressure gradient, and Term VI is viscous dissipation

Following the same methodology, prognostic equations of turbulent flux for scalars can also be found. The turbulent flux of water vapor (q) is shown as the covariance

of q and w components written as:

$$\frac{\partial(\overline{q'w'})}{\partial t} = -\overline{w_2'}\frac{\partial \overline{q}}{\partial z} - \frac{\partial(\overline{q'w'w'})}{\partial z} + (\overline{q'\theta_v'})\frac{g}{\overline{\theta}_v} + \left(\frac{1}{\overline{\rho}}\right)\left[\overline{\rho'\frac{\partial q'}{\partial z}}\right] - 2\epsilon_{wq} \tag{2.3}$$

(I) (II) (III) (IV) (V) (VI)

Analogous to terms in equation 2.2, Term I represents the storage of moisture flux, Term II is the moisture gradient, Term III is the turbulent transport of moisture, Term IV is buoyant production due to moisture, Term V is the pressure redistribution of moisture, and Term VI is the viscous dissipation term (Stull, 1988).

2.3 Flux Measurement

The eddy covariance method allows the measurement of the turbulent motions of the lower atmosphere. These turbulent motions help transport trace gases in the atmosphere, such as CO_2 (Baldocchi, 2003). The instantaneous vertical mass flux density F can be measured to determine the difference of these gases moving past the sensor due to turbulent motion (Baldocchi, 2003). Vertical flux of this turbulent flow can be represented as:

$$F = \overline{\rho_a w s} \tag{2.4}$$

where ρ_a is the density of air and $s = \frac{\rho_c}{\rho_a}$ is the mixing ratio of the measured atmospheric constituent (c). Using Reynolds decomposition to vertical velocity ($w = \overline{w} + w'$) and the scalar mixing ratio (s), equation (2.4) is expanded:

$$F = (\overline{\rho_a w}\,\overline{s} + \overline{\rho}_a\overline{w's'} + \overline{w}\,\overline{\rho_a's'} + \overline{s}\,\overline{\rho_a'w'} + \overline{\rho_a'w's'}) \tag{2.5}$$

Fluctuations of density are assumed to be negligible, therefore, the third, fourth, and fifth terms on the LHS of equation (2.5) are removed. Also, an assumption of eddy covariance is that mean vertical flow is negligible for a horizontal homogeneous surface $\overline{w} = 0$, removing the first term on the LHS yields:

$$F = \overline{\rho_a} \cdot \overline{w's'} \tag{2.6}$$

Equation (2.6) states that mean flux density is the product of the covariance of vertical velocity and scalar mixing ratio. This is generally referred to as the "Eddy Flux" equation.

The mean flux density of the trace gases of interest are typically measured with a standard set of instrumentation. Generally, the main components of an eddy covariance tower include a three-dimensional sonic anemometer and a gas analyzer (Aubinet et al., 2000; Baldocchi et al., 2001b). The three-dimensional sonic anemometer allows the measurement of wind velocities and virtual temperature, while the gas analyzer measures the atmospheric densities of CO_2 and H_2O. The gas analyzers are typically either open or closed path analyzers (Aubinet et al., 2000; Baldocchi et al., 2001b). Other meteorological measurements are also recorded at half hour averages to help characterize the conditions at which the fluxes are measured (Aubinet et al., 2000). These instruments generally include a net radiometer, rain gauge, humidity and temperature sensors, soil moisture, soil temperature, and soil heat flux plates.

2.4 Processing Procedures

The processing steps used in this project are briefly outlined in Baum et al. (2008) and Brunsell et al. (2010a). However this discussion will develop these into an in-depth explanation of the theory behind the methodology and specific procedures that

were conducted. All eddy covariance data was processed by closely following the procedures outlined in Lee et al. (2004) and Mauder et al. (2008).

2.4.1 Spike and Lag Removal

The first step in processing the data is to remove random spikes. These random spikes can be caused by several factors, for example, when water collects on traducers of sonic anemometers during precipitation events (Vickers and Mahrt, 1997). The methodology used to detect spikes and removal follows that of Højstrup (1993), Vickers and Mahrt (1997), and Mauder et al. (2008). The method applies a moving window of a specified size (4 data points) and computes a mean and a standard deviation for the values within the window. The window moves one point at a time until a spike is found. Spikes are determined when the value of the data point exceeds a magnitude of the standard deviation greater than the mean of the window and each variable has a specific threshold. For instance, our coordinate wind measurements (u, v, w) have a threshold of six standard deviations greater than the mean, whereas temperature ($T\,^{\circ}C$) has a threshold of ten standard deviations greater than the mean. Once a data point exceeds the threshold, linear interpolation is used to replace the point. When several consecutive points are detected as exceeding the threshold, then they are no longer considered a spike (Højstrup, 1993; Vickers and Mahrt, 1997).

Lag removal is also performed on the data. This is performed to compensate for the time-delay of data acquisition of the instruments (Aubinet et al., 2000). Generally, this is more of an issue when using a closed-path gas analyzer versus an open-path gas analyzer. If this correction was not applied, turbulent motions would not correlate with fluctuation in gas concentrations, thus making the eddy covariance technique irrelevant. For closed-path analyzers, time lag is typically calculated by optimizing the correlation coefficient of carbon and water densities with the vertical wind velocity

(Haslwanter et al., 2009; McMillen, 1988). For open-path analyzers, minor lag times are induced to reduce flux underestimates. For our purposes, we use a lag correction of 0.33 seconds.

2.4.2 Planar coordinate rotation

Since a sonic anemometer cannot be perfectly level so that w is always perpendicular to the flow, a large error in momentum flux can be attributed to contamination from wind coming in the other two wind components (Wilczak et al., 2001). Therefore, a necessary step in the eddy covariance technique is the process of coordinate rotation (Finnigan, 2004; Finnigan et al., 2003).

A proper coordinate frame must be consistent with the theoretical model framework. The fundamental equation of the eddy covariance technique is the conservation of mass equation (Lee et al., 2004). This is illustrated following the framework of Finnigan (2004) and Lee et al. (2004). The conservation of the scalar (c) at a single point in an incompressible fluid is denoted as:

$$\frac{\partial c}{\partial t} + \nabla \cdot \vec{u}c = S(\vec{x})\delta(\vec{x} - \vec{x_0}) \tag{2.7}$$

where $\vec{u}$ is the velocity vector which contains the u, v, and w components corresponding to position vector $\vec{x}$ with components x, y, z (Finnigan, 2004). The right-hand term in (2.7) is the product of the source term S and the Dirac delta function, which implies that the source is zero except on bare ground and vegetation surfaces (Finnigan, 2004). Although each term is a scalar, the individual terms within the divergence term ($\nabla \cdot (\vec{u}c)$) differ between coordinate systems. Therefore, the interpretation of the conservation of mass on a scalar is dependent on a proper coordinate system that fits the theoretical framework (Finnigan, 2004; Lee et al., 2004).

Coordinate systems describe the balance of mass at a single point by specifying the direction and magnitude of the velocity vector (Lee et al., 2004). The velocity vector in a coordinate system can be written in tensor form as:

$$\vec{u} = u\vec{e_1} + v\vec{e_2} + w\vec{e_3} \tag{2.8}$$

with the velocity vector $\vec{u}$ in the vector basis related to the coordinate lines $\vec{e_i}$ (Lee et al., 2004). In addition to the coordinate system used in the theoretical framework, there is also a coordinate frame deployed by the instrumentation. To reduce airflow interference, transducers of modern anemometers record measurements on a non-orthogonal axis. Therefore, a geometric transformation from the non-orthogonal frame to an orthogonal frame takes place to accurately depict velocity vectors. Once this is accomplished, the $\vec{e_i}$ base vector can be set to a known geographic position (Lee et al., 2004).

The coordinate rotation method used for this study is the planar-fit coordinate (Lee et al., 2004; Paw U et al., 2000; Wilczak et al., 2001). This is the preferred coordinate system for single tower flux measurements (Massman and Lee, 2002). The planar coordinate is a right-handed coordinate where the z coordinate is fixed and the x and y coordinates vary with time. The z-axis is perpendicular to the streamline plane and the y-axis is perpendicular to the short-term (30-min) velocity plane (Lee et al., 2004).

As stated in Lee et al. (2004) and Wilczak et al. (2001), there are three steps involved in converting from instrument coordinate to planar-fit coordinate. This involves rotating the coordinates in sequence by the pitch, roll, and yaw angles. To begin, a time period in which the position of the sonic anemometer did not change must be determined. This time period sould be on the order of weeks or longer. In the next step, one performs a linear regression to define a "tilted" or mean streamline

plane. Following Lee et al. (2004), an alternative approach to Wilczak et al. (2001) using a similar two-dimensional used in Paw U et al. (2000). The unit vector set $\{\vec{i}, \vec{j}, \vec{k}\}$ projects the right-handed orthogonal axes that are parallel to the x, y, and z axes. This leads to the product of $\vec{k}$ and the mean velocity $\vec{\overline{u}}$ as:

$$\overline{w} = \vec{k} \cdot \vec{\overline{u}} \tag{2.9}$$

where $\overline{w}$ is the mean vertical velocity. Substituting the two forms of the instrument coordinate ($\vec{k} = \{k_1, k_2, k_3\}$, $\vec{\overline{u}} = \{\overline{u_1}, \overline{v_1}, \overline{w_1} - b_0\}$) into Equation (2.9) yields:

$$\overline{w_1} = b_0 + b_1\overline{u_1} + b_2\overline{v_2} + \overline{w}/k_3 \tag{2.10}$$

where b_0, b_1, and b_2 are regression coefficients, the last term represents "random noise" and $\overline{u_1}$,$\overline{v_1}$, $\overline{w_1}$ are the components of the mean wind (Lee et al., 2004). Once the regression coefficients (b_1 and b_2) are known, the yaw and roll angles can be calculated for rotation (Lee et al., 2004).

2.5 Sampling Corrections

It is widely known that eddy covariance systems attenuate turbulent signals at both the high and low frequencies (Massman, 2000; Massman and Lee, 2002; Moore, 1986). This signal loss is attributed to several sources, including instrument limitation, instrument separation, time response, and signal processing (Massman, 2000; Massman and Lee, 2002; Moore, 1986). Although these systems are prone to attenuation, there are a variety of methods to help minimize and correct flux losses.

2.5.1 Frequency Response Corrections

High/Low-Pass Filtering

When applying Reynolds averaging, de-trending, or non-linear filtering to sampled measurements, high frequency fluctuations in the co-spectrum are passed, but low-frequency fluctuations are attenuated (Moore, 1986). Therefore, this results in a loss of flux. To compensate for this loss, a high-pass filter correction can be applied to the data. Following Moore (1986), the transfer function for a high-pass filter Υ_{hi} correction is denoted as:

$$\Upsilon_{hi}(n) = 2\pi\tau_f \left(\frac{1 + \frac{(2\pi n\tau_f)^2}{1}}{(1 + \frac{1}{\tau_f n_c})} \right)^{-1.5} \tag{2.11}$$

where n is frequency, n_c is the Nyquist frequency, and τ_f is the high pass filter constant (Moore, 1986). Fluxes may also be lost in the high frequency fluctuations due to anti-aliasing filters. Therefore, low-pass filter corrections may also be used. The low-pass filter Υ_{lo} is written as (Moore, 1986):

$$\Upsilon_{lo}(n) = 1 - \Upsilon_{hi}(n) \tag{2.12}$$

Digital Sampling

Eddy covariance systems take discrete digital samples at high frequencies n_s, generally at 10 or 20 Hz. However, since discrete samples are conducted at specific intervals, small fractions of seconds occur between measurements. This causes the high frequency contributions to appear at lower frequencies, or what is referred to as aliasing (Moore, 1986). When aliasing occurs the high frequency signals are lowered between 0 and half of n_s, or the Nyquist frequency. To compensate for aliasing during

sampling, Moore (1986) proposes the transfer function for digital sampling Υ_{ds} as:

$$\Upsilon_{ds}(n) = 1 + \left(\frac{n}{n_s - n}\right)^3 \tag{2.13}$$

This correction is only valid for frequencies less than or equal to the Nyquist frequency, $n \leq n_s/2$. Applying this correction below the Nyquist frequency avoids aliasing in high frequencies above $n_s/2$ (Moore, 1986).

Sensor Path Averaging

The sonic anemometers and open-path infrared gas analyzers in an eddy covariance system have finite sensor paths. Turbulent fluxes are underestimated due to the loss of small eddies as samples are averaged across the sensor path. Therefore, Moore (1986) outlines the transfer function for scalar path averaging Υ_{sp} correction as:

$$\Upsilon_{sp}(n) = \left(\frac{3 + exp(-2\pi n\frac{x_s}{u} - (\frac{4}{2\pi n\frac{x_s}{u}})(1 - exp(-2\pi n\frac{x_s}{u}))}{2\pi n\frac{x_s}{u}}\right)^{-1/2} \tag{2.14}$$

where x_s is the scalar path length (Moore, 1986).

Sensor Separation

The horizontal separation of the two instruments attributes to flux loss due to the inability of the sensors to accurately measure horizontal velocities and scalar quantities within the same volume (Moore, 1986). This applies specifically to scalar fluxes, but not to fluxes of sensible heat or momentum (because these fluxes are determined solely from the sonic anemometer). The sensor separation correction is displayed by

the transfer function Υ_s as:

$$\Upsilon_s(n) = e^{-9.9(nx_d/u)^{1.5}} \tag{2.15}$$

where x_d is the distance between sensors (Moore, 1986).

2.5.2 Webb-Pearman-Leuning Corrections

Webb et al. (1980) discussed the need to correct eddy covariance measurements using open path gas analyzers, because of fluctuations in water vapor ($\overline{w'q'}$) and temperature flux ($\overline{w'T'}$), which have an effect on flux estimations of the atmospheric scalar c (Aubinet et al., 2000; Lee et al., 2004; Leuning, 2007; Webb et al., 1980). The original theory proposed by Webb et al. (1980) applied to one-dimensional flow over a flat, homogeneous terrain. Therefore, this idea might not be suitable for measurements placed in non-flat, heterogeneous areas (Lee et al., 2004). The original correction proposed by Webb et al. (1980) is written as:

$$F_c = \overline{w'\rho_c'} + \frac{m_a}{m_v}\frac{\overline{\rho_c}}{\overline{\rho_a}}\overline{w'\rho_v'} + \left(1 + \frac{\overline{\rho_v}m_a}{\overline{\rho_a}m_v}\right)\frac{\overline{\rho_c}}{\overline{T}}\overline{w'T'} \tag{2.16}$$

where m_a and m_v are the molar masses of dry air and water vapor, respectively (Baldocchi, 2003). Several assumptions are made in deriving Equation (2.16). The equation neglects fluctuations in pressure, which may be problematic in high wind conditions (Baldocchi, 2003; Massman and Lee, 2002), and neglects the covariance of temperature and pressure (Baldocchi, 2003; Fuehrer and Friehe, 2002). According to Paw U et al. (2000), the derivation also neglects advection, which is important when dealing with sloping surfaces (Baldocchi, 2003).

Unlike closed-path gas analyzers, open-path gas analyzers cannot simultaneously measure temperature and pressure at the same sampling frequency as measurements

of concentrations of H_2O or CO_2. Therefore, open-path gas analyzers are unable to calculate mixing ratios similar to that of closed-path gas analyzers (Lee et al., 2004). Due to this fact, when using open-path gas analyzers, the corrections of Webb et al. (1980) must be applied to sensible heat and water vapor fluxes. Sensible heat flux can be calculated using the thermometers on a sonic anemometer (Schotanus et al., 1983). Using the temperature calculated by the sonic anemometer T_s, the sensible heat flux can be written as:

$$\overline{w'T'_s} = \overline{w'T'} + 0.51\overline{T}\ \overline{w'q'} - 2\frac{\overline{T}\bar{u}}{c^2}\overline{u'w'} \tag{2.17}$$

Now, water vapor flux can now be calculated using the Webb et al. (1980) corrections. The water vapor flux density is written as (Lee et al., 2004):

$$F_{H_2O} = \left(1 + \frac{\overline{\rho_v}m_a}{\overline{\rho_a}m_v}\right)\left(\overline{w'\rho'_v} + \overline{\rho_v}\frac{\overline{w'T'}}{\overline{T}}\right) \tag{2.18}$$

2.6 Quality Control

An important step in the eddy covariance data collection is quality control. Quality control of eddy covariance measurements test for faulty instrumentation and errors, as well as how closely conditions follow the underlying theory (Foken et al., 2004). The methodology used to conduct quality control filtering closely follows that of Hammerle et al. (2007) and Foken and Wichura (1996). Using half-hourly averaged flux data, an integral turbulence test and stationarity test is performed.

2.6.1 Integral Turbulence Test

To assess the deviation from Monin-Obukhov (MO) similarity theory, the integral turbulence test is used (Hammerle et al., 2007). Following Kaimal and Finnigan

(1994), the similarity function for vertical wind velocity (ϕ_w) is computed as the ratio of the standard deviation of vertical wind velocity (σ_w) and friction velocity (u_*):

$$\phi_w = \frac{\sigma_w}{u_*} = \begin{cases} 1.25(1+3|z/L|)^{1/3}, & -2 \leq z/L < 0 \\ 1.25(1+0.2z/L), & 0 \leq z/L < 1 \end{cases} \tag{2.19}$$

where z is the measurement height and L is the Obukhov length (Stull, 1988). The percentage difference between the observed similarity function and the modeled similarity function is shown in the ∇_{ITT}. Any values greater than 30% are excluded from the analysis. The ∇_{ITT} is written as :

$$\nabla_{ITT} = \frac{100|(\sigma/u_*) - \phi_w|}{\phi_w} \tag{2.20}$$

2.6.2 Stationarity test

Deviations from stationarity are assessed using half-hourly averages of the covariances of vertical velocity and scalar mixing ratios ($\overline{w's'}$) (Hammerle et al., 2007). Differences in stationarity (∇_{ST}) are calculated as:

$$\nabla_{ST} = \frac{100|\overline{w's'_5} - \overline{w's'_{30}}|}{\overline{w's'_{30}}} \tag{2.21}$$

where the 5 and 30 subscripts denote 5- and 30-min covariances (Hammerle et al., 2007). Values of ∇ST 30% or greater are removed from analysis.

2.7 Issues with Spatial Heterogeneity

The spatial heterogeneity of the land surface has been found to influence flux measurements (Schmid and Lloyd, 1998). Using a footprint model can be a useful tool to assess the upwind area contributing to flux estimates. The tower footprint provides

the "field of view" of surface-atmosphere exchange (Schmid, 2002). The size and extent of a footprint is dependent on such factors as the atmospheric stability, measurement height and surface roughness (Hsieh et al., 2000). Nighttime meteorological conditions often create large footprint areas that can extend beyond the surface under investigation (Aubinet, 2008; Massman and Lee, 2002). Therefore location of the sensor, as well as land cover variability can have a profound impact on flux estimates (Schmid and Lloyd, 1998).

Another well-documented issue when using the eddy covariance technique is the energy balance closure problem (Twine et al., 2000; Wilson et al., 2002). It has been found that fluxes sampled by eddy covariance systems do not conserve energy, with the turbulent fluxes being approximately 70% of the available energy (Wilson et al., 2002). Proposed causes of this phenomena are reviewed in Foken et al. (2006). Studies conducted by Inagaki et al. (2006) and Panin et al. (1998) have associated the lack of energy balance closure with spatial heterogeneity across the and surface. These studies have suggested that the heterogeneity of the surface modified the turbulent structure of the lower atmosphere, generating eddies at larger timescales than measured with the eddy covariance method. This has also been shown using large eddy simulations over heterogeneous surfaces (Huang et al., 2009).

2.8 Issues with Long-Term Measurements

When dealing with long-term (on the order of 1 year or more) eddy covariance measurements, it is inevitable to have gaps within the data. This may occur as a result of prescribed fire burns, routine maintenance, complete system failure, faulty instrumentation, and instrumentation damage due to storms or animals, or failing stationarity and ITT tests. Several approaches to gap-filling are outlined in papers from Moffat

et al. (2007), Falge et al. (2001), and Aubinet et al. (2000). Examples of gap-filling strategies include interpolation, parameterization, or linear regression (Aubinet et al., 2000).

The current gap-filling strategy used in this project consisted in a moving window to calculate diurnal mean averages of fluxes. An adaptive window size based on the gap size is used for mean averaging. However, after analysis it was determined that these gap-filled values are unreliable. Variabilities in carbon and water fluxes were filtered, even though they were deemed to be reasonable measurements. Consequently, gap-filled data was not used in the study outlined in the following chapter.

2.9 Summary

The eddy covariance method has proven to be a useful tool in assessing the exchange of energy and mass between the surface and the atmosphere. However instrumentation error, instrument limitations, and physical environmental conditions have been attributed to errors in flux measurements. In this chapter we examined the underlying theory of eddy covariance, as well as specific post-data collection processing procedures. These procedures included spike and lag removal, planar coordinate rotation, frequency response corrections, and Webb-Pearman-Leuning corrections.

Quality-control tests were conducted on data to further test for instrumentation errors. This included a Monin-Obukhav stationarity test and integral turbulence test. Gap-filling strategies for long-term data sets were also discussed. However, it was concluded that the current gap-filling strategy being used was unfit, and needed further analysis. The impact of spatial heterogeneity on measured footprint area and energy balance closure was also discussed.

Chapter 3

Impacts of seasonality and surface heterogeneity on water-use efficiency in grasslands

3.1 Introduction

Understanding how ecosystems respond to climate and land-cover change for both present and future conditions is a concern amongst many people due to the ecological, social, economic, and political impacts it may have on human society (Dale, 1997). Of the world's ecosystems, grasslands cover nearly 40% of the Earth's terrestrial surface (Emmerich, 2007; Novick et al., 2004) and account for 30 to 35% of the global net primary production (Archer et al., 2001). Several studies have shown that grasslands are extremely susceptible to climate change (Brunsell et al., 2010b; Burke et al., 1991; Hopkins and Del Prado, 2007; Soussana and Lüscher, 2007). One of the possible impacts of climate change on these ecosystems is the potential for changing carbon source/sink dynamics (Hall et al., 1995; Scurlock and Hall, 1998; Thornley

and Cannell, 1997). Predicted increases in temporal variability of precipitation have also been shown to increase plant water stress and alter carbon cycling processes in grasslands (Knapp et al., 2002). Due to the vast amount of the Earth's surface occupied by grasslands, it is important to understand the effects of climate change on grasslands and its possible impact on global carbon and water cycling.

Although there has been much emphasis on the effect of climate change on grasslands, the impact of land-cover and land-use change must be understood as well. The fraction of the Earth's surface, including grasslands, that have undergone anthropogenic land cover change is estimated to be on the order of 39 to 50% (Vitousek et al., 1997). Historically, land-cover and land-use change in central plains grasslands has been primarily due to the conversion of native grasslands into agricultural use (Briggs et al., 2005). However, grasslands currently are threatened by the invasion of woody plants, also known as woody encroachment (Briggs et al., 2005; Scott et al., 2006). Grasslands, such as tallgrass prairie, lie in regions that exhibit favorable conditions for transitions from grasslands to forests. This is due to the fact that these grasslands exist in the region between arid grasslands and mesic forests (Briggs et al., 2005). There have been several factors that have been attributed to the invasion of woody-plants, including fire suppression, introduction of grazing livestock, elimination of native fauna, and invasive species of plants (Briggs et al., 2005; Burkinshaw and Bork, 2009; Scott et al., 2006) as well as climate change (Eggemeyer and Schwinning, 2009). Increases in woody-vegetation in grassland ecosystems have been found to alter biochemistry of ecosystems by increasing carbon storage (Archer et al., 2001; McKinley and Blair, 2008). These sites also experienced increased evapotranspiration due to increases in woody-vegetation (Scott et al., 2006) and ecohydrological alterations by decreases in available soil water (Huxman et al., 2005; Jackson et al., 2007).

Grasslands are generally resource limited due to water availability (Ojima et al., 1993). An appropriate method of examining carbon and water cycling, therefore would be to evaluate the efficiency. Water-use efficiency (λ) is defined as the as the cost of carbon in units of water (Buckley et al., 2002). The actual definition of λ depends on the spatial scale of examination. At the leaf-level, λ is the ratio of the amount of carbon assimilated to the amount of water transpired through the stomata (Buckley et al., 2002; Cowan and Farquhar, 1977). At this scale, λ is regulated by the maximum measurable amount of water and carbon released by the leaf, or stomatal conductance, since it limits the transpiration loss more than carbon assimilation (Ponton et al., 2006).

When scaling from leaf to an ecosystem there are additional factors in hand that affect the interpretation of λ. In addition to transpiration from the stomata, the evaporation of soil or surface water must also be taken into account (Ponton et al., 2006). Ecosystem λ may also vary due to species composition (Emmerich, 2007; Monson et al., 1986). Therefore, ecosystem-scale λ is generally calculated as the ratio between either net primary production (NPP), net ecosystem production (NEP), or gross primary production (GPP) to water-loss (Kuglitsch et al., 2008).

Variability in λ may also be seen across different timescales. Different mechanisms, such as precipitation variability or temperature trends over different timescales may produce different values of λ (Kuglitsch et al., 2008). Seasonal and inter-annual variations in temperature and precipitation have been found to alter ecosystem carbon allocation (Flanagan et al., 2002; Xu and Baldocchi, 2004). Variability in values of λ during shorter timescales (i.e., daily) may be overridden when averaging over larger time scales (i.e., annual) (Beer et al., 2009). Understanding how λ varies over different timescales may give insight to the possible trends seen within the data.

With this purpose in mind, the eddy covariance method has proved to be a con-

venient method of measuring and assessing carbon and water cycling. The eddy covariance method allows direct measurement of the exchanges of carbon and water between the surface and the atmosphere (Baldocchi et al., 2001a). Therefore, λ can be evaluated directly at the ecosystem scale (Kuglitsch et al., 2008; Law et al., 2002). Since eddy covariance systems do not directly measure carbon assimilation, this value is derived from measurements of net ecosystem exchange (NEE) (Beer et al., 2009).

The main focus of this study is to examine how land-cover in central plains grasslands affects carbon and water cycling. Specifically how λ varies across different land-cover regimes (i.e. vegetation composition), precipitation gradients, and by daily, monthly, seasonal and inter-annual scales. The main objectives of this study are to use the eddy covariance technique to: 1) examine how λ efficiency varies between sites with homogeneous land-cover composition and sites experiencing woody encroachment 2) examine the impact of land-cover variability on the relationship between λ and site-specific variables (e.g. soil moisture, temperature, and precipitation) 3) assess how temporal variability of λ varies across land-cover type. Understanding these concepts will give a better idea of how similar ecosystems will respond to land-cover and climate changes in the future.

3.2 Methods

3.2.1 Site Description

For this study, three different grasslands in northeastern Kansas were used. The Nelson Environmental Research Area (NESA) study site, is located 8 km north of Lawrence, Kansas (39°N, 94°W) (Billings, 2006; Fitch and Kettle, 1988). NESA is part of the University of Kansas Field Station (KUFS). NESA lies on the ecotone between the eastern edge of the tall grass prairie and the western edge of the east-

ern deciduous forest biomes (Billings, 2006). The area experiences a mid-continental climate with a mean annual temperature of 13.3°C. The site experiences an average growing season of 185 days and mean annual precipitation of 937 mm (Billings, 2006; Brunsell et al., 2010a). The tower is located on restored prairie that was used extensively as agricultural land between the 1940s and the 1960s, and was a hay field until 1987. Maintenance includes periodic burning approximately every three years and mowing. Currently, the study area contains a mixture of C_3 and C_4 grasses and is experiencing woody encroachment (Brunsell et al., 2010a).

The remaining two grasslands are located at the Konza Prairie Biological Station (KPBS), located approximately 8 km south of Manhattan, Kansas (39°N, 96°W) (Nippert et al., 2009), approximately 115 km west of NESA. KBPS is located in the Flint Hills region of Kansas and is also characterized as having a mid-continental climate (Nippert and Knapp, 2007) and a mean annual temperatures of 13°C (Collins, 1992). KPBS experiences a growing season between April and September and has an mean annual precipitation of 835 mm (Hayden, 1998; Nippert et al., 2009). The first site at KPBS is located in an annual burned, non-grazed watershed in an upland area (KZU). The KZU site is primarily dominated by native C_4 grasses (Nippert and Knapp, 2007) and has been burned annually since 1978 (http://www.konza.ksu.edu/old_web/UltraDev/Search.asp?currMenu=57&depth=2). The second study site (K4B) is also primarily dominated by native C_4 grasses, but is experiencing woody encroachment. From 1975-2009, the watershed had prescribed burns every four years, but also experienced unprescribed wildfires in 1994 and 2000 (http://www.konza.ksu.edu/old_web/UltraDev/Search.asp?currMenu=57&depth=2).

3.2.2 Field Measurements

Field measurements at all sites were conducted using the eddy covariance technique (Baldocchi et al., 2001a). Field measurements at NESA were taken from June 21 (DOY 167), 2007 to December 31 (DOY 365), 2009; KZU measurements were conducted from August 2 (DOY 214), 2006 to December 31 (DOY 365), 2009, and K4B measurements were conducted from May 7 (DOY 127), 2007 to December 31(DOY 365), 2009.

Net ecosystem exchange (NEE), water flux (LE), and sensible heat (H) measurements were conducted with a Campbell Scientific CSAT3 3D Sonic Anemometer and a LICOR 7500 Open-Path Gas Analyzer. Both flux instruments were located on the tower 3.0 m above the surface. The sonic anemometer was used to measure wind direction and turbulent fluctuations of wind velocities and virtual temperature. The open-path gas analyzers measured gas concentrations of CO_2 and water vapor in the atmosphere and was inclined to 15° into the mean wind direction to reduce any radiation effects on the sensor (Ham and Heilman, 2003). Energy balance measurements included soil heat flux (G) and net radiation (Rn). For soil heat flux, soil heat flux plates were installed 8 cm below the surface, while thermal couples are installed above the soil heat flux plate at 2 cm and 6 cm soil depths. Net radiation measurements are conducted with a net radiometer, including a REBS Q7.1 Net radiometer (NESA: DOY 167, 2007 - DOY 324, 2009; KZU: DOY 138, 2007 - DOY 118 2009; K4B: DOY 124 2007 - DOY 113 2009), Kipp and Zonen CNR1 four-way net radiometer (NESA: DOY 324 2009-Present), and a Kipp and Zonen CNR2 four-way net radiometer (KZU: DOY 118 2009 - Present; K4B: DOY 113 2009 - Present). All net radiometers were placed approximately 2 m above the surface. Net radiometer measurements are missing at NESA between October 15, 2007 and Novemeber 14, 2007 due to a bird attack on the sensor. Ancillary meteorological data also col-

lected at these sites include precipitation, temperature and humidity, photosynthetic active radiation (PAR), and soil moisture. Measurements were sampled and stored using Campbell Scientific dataloggers, including CR23X (KZU, K4B), CR1000 (KZU, K4B), and CR3000 (NESA). Turbulent measurements were collected at 20 Hz, while ancillary data were stored at 30 minute averages.

3.2.3 Data Processing

Several post-data collection processing methods were used on the 20 Hz data from each site. This methodology closely follows the data processing outlined in Baum et al. (2008) and Brunsell et al. (2010a). All 20 Hz data collected from the eddy covariance towers was processed with the EdiRE software package (Clement, 1999). Corrections on the 20 Hz data included despiking, lag removal and planar-fit rotation (Paw U et al., 2000), frequency-response corrections (Moore, 1986), sonic-temperature sensible heat flux corrections (Schotanus et al., 1983), and density corrections for carbon and water fluxes (Webb et al., 1980). EdiRe was used to calculate other parameters, such as Obukhov length (L), stability parameters (z/L), and friction velocity (u_*) (Baum et al., 2008). After data was processed with EdiRe, quality-control filtering was performed using MATLAB® code (The MathWorks, 2008). Quality-control filtering methodologies similar to those outlined Foken and Wichura (1996) and Hammerle et al. (2007) were conducted on the 20 Hz data collected from all sites. Two tests were used to filter data, including an integral turbulence test and a stationarity test (Hammerle et al., 2007). An integral turbulence test is a comparison of the vertical windspeed to the friction velocity (σ_w/u_*). Values greater than 30% were removed. The stationarity test examined six covariance intervals. Any of the intervals differing more than 60% were removed (Foken and Wichura, 1996; Hammerle et al., 2007). Filtered and missing data is generally gapfilled for continuous sets of

data. However, due to uncertainties within the gapfilled values, only actual measured values were used for this data analysis.

3.2.4 Water-Use Efficiency

Water-use efficiency (λ) can be defined as the ratio of the amount of carbon vegetation assimilates to the amount of water lost (Baldocchi, 1994). To find λ, ecosystem respiration (R_{eco}) must be caluclated. To caluclate R_{eco}, only nighttime values are examined (Falge et al., 2002). Stability parameters for nighttime unstable conditions ($z/L < 0.1$) and reasonable turbulence ($u_* > 0.15$) were used to identify periods to be used to estimate respiration via a Q_{10} temperature coefficient (Lloyd and Taylor, 1994):

$$R_{eco} = R_{10} Q_{10}^{(T-10)/10} \tag{3.1}$$

where R_{10} is a coefficient of least squares regression and T is air temperature in °C (Falge et al., 2002). This relationship is then applied to all half-hour periods at each sites to calculate ecosystem respiration. Once half-hour R_{eco} values were determined, carbon assimilation (A) was calculated as:

$$A = NEE - R_{eco} \tag{3.2}$$

water-use efficiency can be found by determining the slope of a linear regression between A and LE (Baldocchi et al., 2001a; Brunsell et al., 2010a):

$$\lambda = dA/dLE \tag{3.3}$$

As plants assimilate carbon, negative values of NEE result in negative values of A. This means that as the ecosystem becomes more efficient at assimilating carbon

per-unit of water, λ values decrease. Positive values of λ would indicate periods of ecosystem respiration. Generally, the majority of these values take place during the late autumn, winter, and spring months and were filtered from our analysis.

Averages of λ were also calculated at multiple timescales. Daytime 30-minute averages of LE and A were used to calculate daily, monthly, and annual averages of λ via linear regression. A five-day window of LE and A values was used to calulate a five-day moving average of λ.

3.2.5 Energy Balance Closure

The eddy covariance method allows independent measurements of all of the major flux components of the energy balance (Twine et al., 2000; Wilson et al., 2002). The radiation balance is stated as:

$$Rn = H + LE + G + S + Q \tag{3.4}$$

where S ($\mathrm{W\,m^2}$) is the canopy heat storage, and Q ($\mathrm{W\,m^2}$) is any additional energy sources or sinks. Q is generally neglected due to its small value (Wilson et al., 2002). However, it has been found that these measurements do not hold to the conservation of energy (Foken et al., 2009; Twine et al., 2000; Wilson et al., 2002). The ratio of energy the turbulent fluxes to the available energy gives a measure of this imbalance:

$$EBR = (H + LE)/(Rn - G) \tag{3.5}$$

Perfect energy balance closure would consist of a ratio of EBR = 1. Here, EBR was used to assess to what extent there was a relationship between closure in different land-cover regimes and water-use efficiency.

3.3 Results

Energy balance and scalar fluxes were analyzed to assess the effect of land cover between the sites (Figure 3.1). Peak Rn values ($\sim$700 $\mathrm{W\,m^{-2}}$) appear to have little variation from site to site. Peak latent heat flux values for both KZU and K4B appear to be greater than the NESA site ($\sim$800 $\mathrm{W\,m^{-2}}$ vs. $\sim$600 $\mathrm{W\,m^{-2}}$). KZU and K4B received greater amounts of precipitation than NESA (Table 3.1). From Table 3.1, mean temperatures for KZU and K4B were higher than NESA. Both higher annual precipitation and higher mean temperatures at KZU and K4B help to explain the higher values in LE. This may also explain the higher peak H values that appear at both KZU ($\sim$420 $\mathrm{W\,m^{-2}}$) and K4B ($\sim$460 $\mathrm{W\,m^{-2}}$) sites compared to NESA ($\sim$343 $\mathrm{W\,m^{-2}}$). Soil heat flux (G) values appear to be higher at the KZU site during the early spring months than at the other two sites. This appears to be in response to the annual burning that takes place at KZU ($\sim$125 $\mathrm{W\,m^{-2}}$) in mid-late April. Burned biomass lowers surface albedo, which in turn increases G. Carbon flux values indicate that all sites were carbon sinks. Both KZU and K4B sites showed much more dramatic carbon uptake than the NESA site, which had consistently lower values of NEE during the growing seasons.

The effect of land cover on water-use efficiency was examined on several parameters, including soil moisture (θ), and energy balance closure. Figure 3.2 shows the five-day mean λ as a function of θ. Soil moisture values vary from 0.17-0.48 $\mathrm{m^3\,m^{-3}}$ at NESA, 0.18-0.57 $\mathrm{m^3 m^{-3}}$ at KZU, and 0.14-0.49 $\mathrm{m^3\,m^{-3}}$ at K4B. Interestingly, there appears to be no significant relationship between λ and θ. As shown in Figure 3.2, there appears to be little or no trend in λ due to variability in θ.

The impact of land cover on contributing source area was examined by using the footprint model of Hsieh et al. (2000). According to this model, footprint area is a

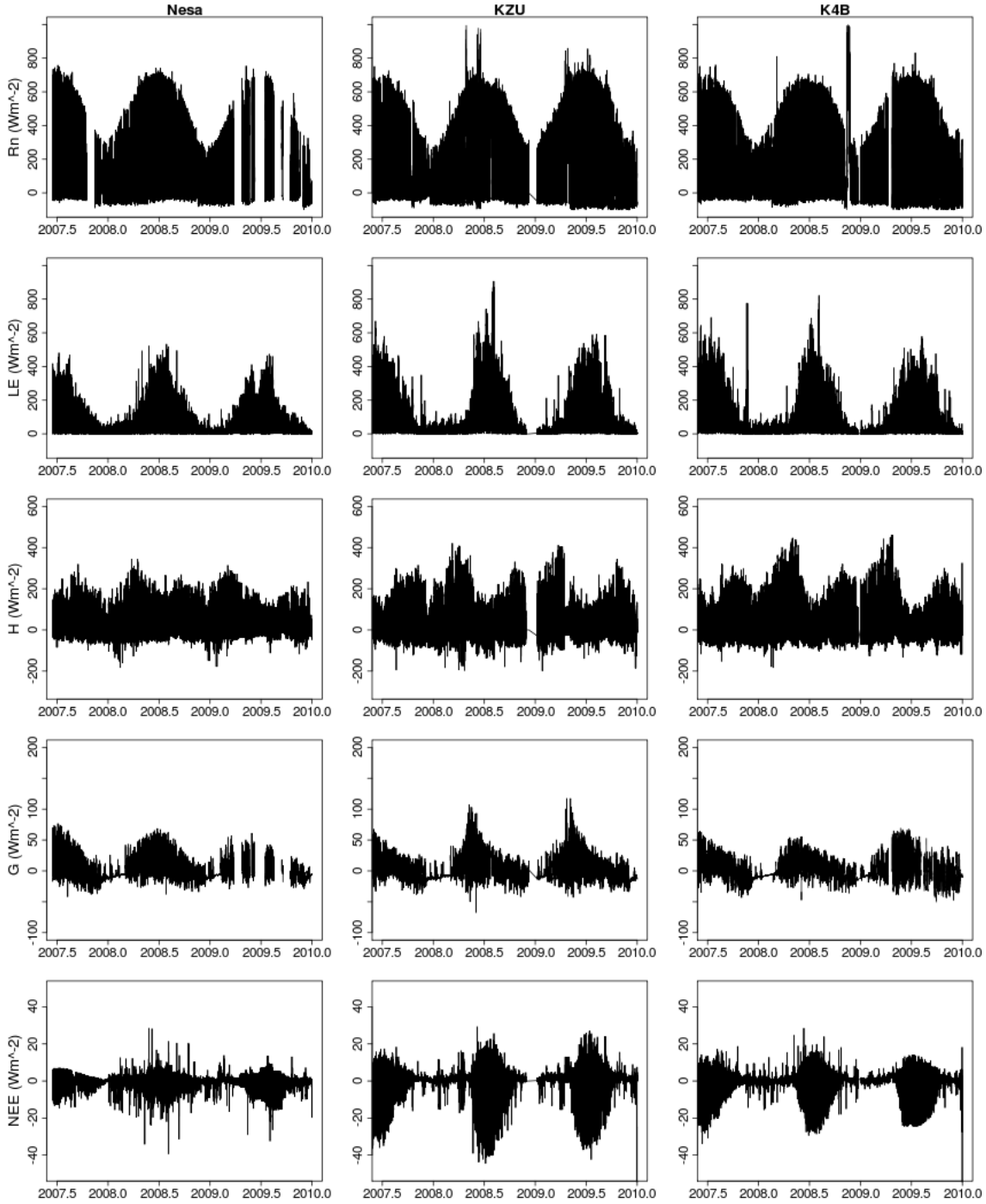

Figure 3.1 Time-series of (in order from top to bottom) net radiation (Rn), latent heat flux (LE), sensible heat flux (H), soil heat flux (G), and net ecosystem exchange (NEE) for NESA (left column), KZU (middle column) and K4B (right column) study sites.

Table 3.1 Annual averages for NESA, KZU and K4B study sites. (Annual mean temperature and precipitation are the same for KZU and K4B).

	NESA			**KZU**			**K4B**		
	2007	**2008**	**2009**	**2007**	**2008**	**2009**	**2007**	**2008**	**2009**
Temperature (°C)	13.3	12.8	12.2	14.9	13.8	14.0	14.9	13.8	14.0
Precipitation (mm)	982.6	1049.6	1062.2	992.6	1073.9	1054.6	992.6	1073.9	1054.6
Rn ($\mathrm{W\,m^{-2}}$)	109.1	88.8	73.2	100.9	92.9	92.1	113.4	102.3	86.2
LE ($\mathrm{W\,m^{-2}}$)	59.4	52.7	38.9	54.7	52.4	49.4	71.3	50.1	47.7
H ($\mathrm{W\,m^{-2}}$)	21.8	21.5	21.9	21.0	18.6	20.1	18.9	24.0	22.1
G ($\mathrm{W\,m^{-2}}$)	-1.65	-0.13	-1.85	-0.92	-0.75	-1.37	-0.75	-0.69	-2.05
NEE ($\mathrm{W\,m^{-2}}$)	0.03	-0.35	-0.49	-0.60	-0.52	-0.72	-0.96	-0.95	-1.40
Bowen Ratio	0.61	0.66	0.56	0.90	0.54	0.46	0.49	0.55	0.48
λ	-17.9	-15.4	-14.2	-8.2	-7.7	-7.2	-12.3	-10.5	-8.2
Spring λ	-26.8	-16.9	-19.7	14.9	-7.9	-7.1	-7.7	-11.6	-6.9
Summer λ	-23.1	-22.2	-21.6	-11.4	-8.9	-7.8	-14.9	-11.3	-10.3

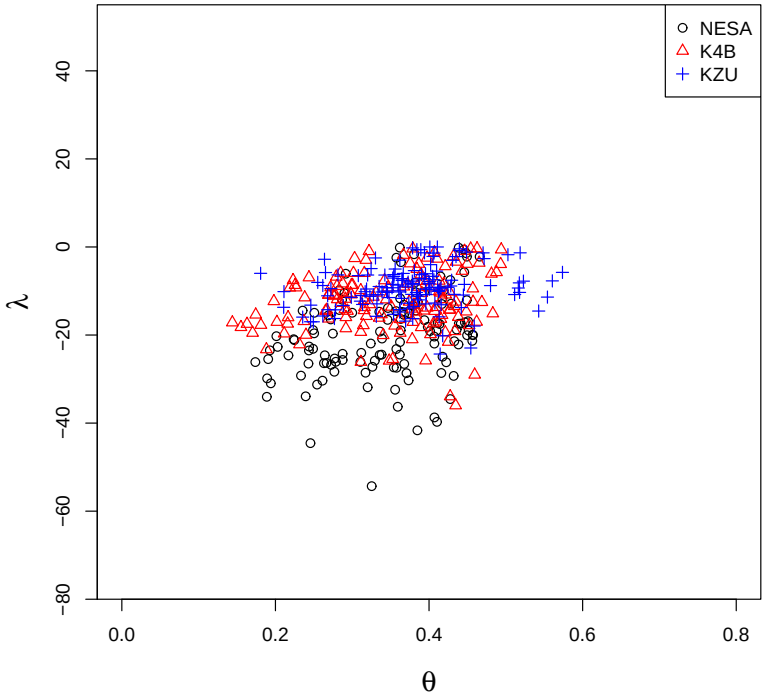

Figure 3.2 Five-day mean water-use efficiency (λ) as a function of five-day mean soil moisture (θ).

function of atmospheric stability, measurement height and surface roughness. Fetch distance was calculated for 70% flux source contribution. Greater fetch values were generally seen for the KZU site, with most values ranging between 200-300 m. At NESA, most values ranged from 150-250 m, and at K4B between 100-200 m. Fetch values were compared to λ to investigate whether there is a relationship between fetch distance and the efficiency of vegetation. Although it appeared that homogeneous surfaces, such as KZU showed larger fetch distances and less efficient water-use values, compared to the two other sites that contain more heterogeneous surfaces and more efficient water-use values, there was not enough evidence to conclude a relationship (data not shown).

Energy balance closure was calculated at five-day averages. Generally, for all sites

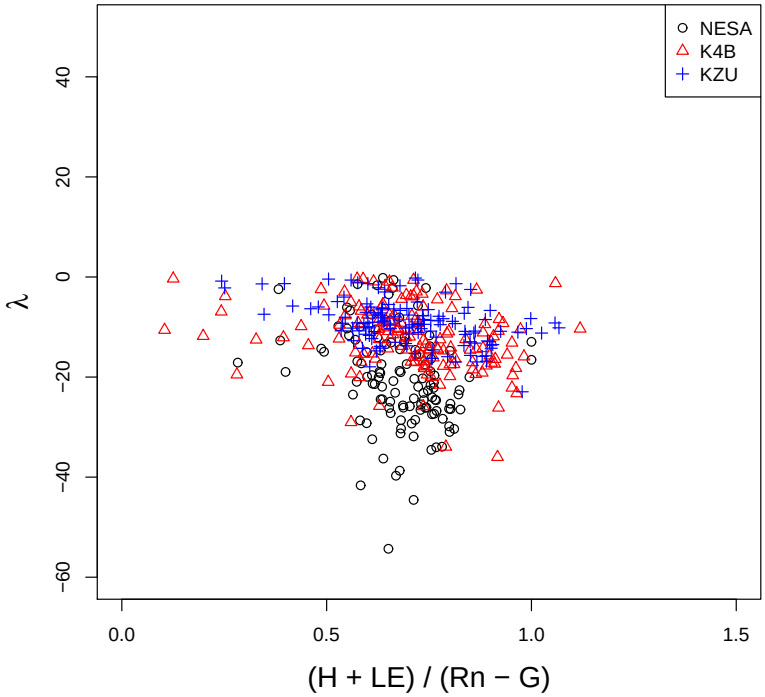

Figure 3.3 Five-day mean water-use efficiency (λ) as a function of energy balance closure.

the majority of closure values fell between 0.5 and 1.0. KZU and K4B both appeared to have a greater amount of closure (values closer to 1) than NESA. Five-day averaged closure values were compared to five-day averaged λ (Figure 3.3). This was conducted to examine if there was a relationship between energy balance closure and λ. When comparing theses two variables there does not appear to be a correlation between variability in energy balance closure and λ across differing land cover.

To assess the effect of seasonality on λ, mean values for daily, five-day, monthly, Spring, Summer, and annual timescales were calculated. From daily and five-day average λ values (Figure 3.4), seasonal variation of λ within the sites can be seen throughout the year. During the growing season λ values decrease until the summer months, when efficiency is at its peak. This may be attributed to the fact that

vegetation would be assimilating carbon more efficiently when photosynthesis is at its peak, or that this may be a seasonal trend in LE which would then affect the carbon assimilation rate in plants. Generally, less negative values of λ were observed at the KZU site. Values of λ for NESA and K4B sites tend to be within the same proximity, however NESA displays more negative values. This is especially pronounced when examining mean seasonal and annual values at NESA, which has lower λ values compared to KZU and K4B (Table 3.1).

Across all sites, there is an increase in λ when examining mean annual values, indicating that the efficiency of plants assimilating carbon decreased from 2007 - 2009 (Figure 3.4). Similar trends can be seen by examining mean spring and summer values (Figure 3.5). Mean spring values indicate an increase in λ at K4B (2007: -13.8; 2008: -11.6; 2009: -6.9), while KZU values stay relatively constant (2007: -7.9; 2008: -7.1; 2009: -7.7). However, NESA showed a decrease in efficiency from 2007 (-16.9) to 2008 (-26.8), then an increase in efficiency in 2009 (-19.7). Similar to annual mean values, mean summer values also show an increase in λ for all sites. The 2009 year was an interesting case because all three sites experienced prescribed burns (Figure 3.6). For a few months following the burn, NESA exhibits much more efficient water-use compared to previous years, while KZU showed values are on par with previous years, and K4B showed less negative values of λ compared to previous years.

In order to assess the impact of seasonality on energy partitioning between the sites, mean annual Bowen ratios (H/LE) were evaluated (Figure 3.7). The NESA site displayed the highest mean annual Bowen ratio (Table 3.1). K4B initially saw the lowest values in 2007, however in 2008 and 2009 KZU had lower Bowen Ratio values. Variability in precipitation appears to be the primary factor for variations in Bowen ratio due to vegetation composition, while inter-annual variations for NESA and K4B may be due to heterogeneous species composition. This will be covered

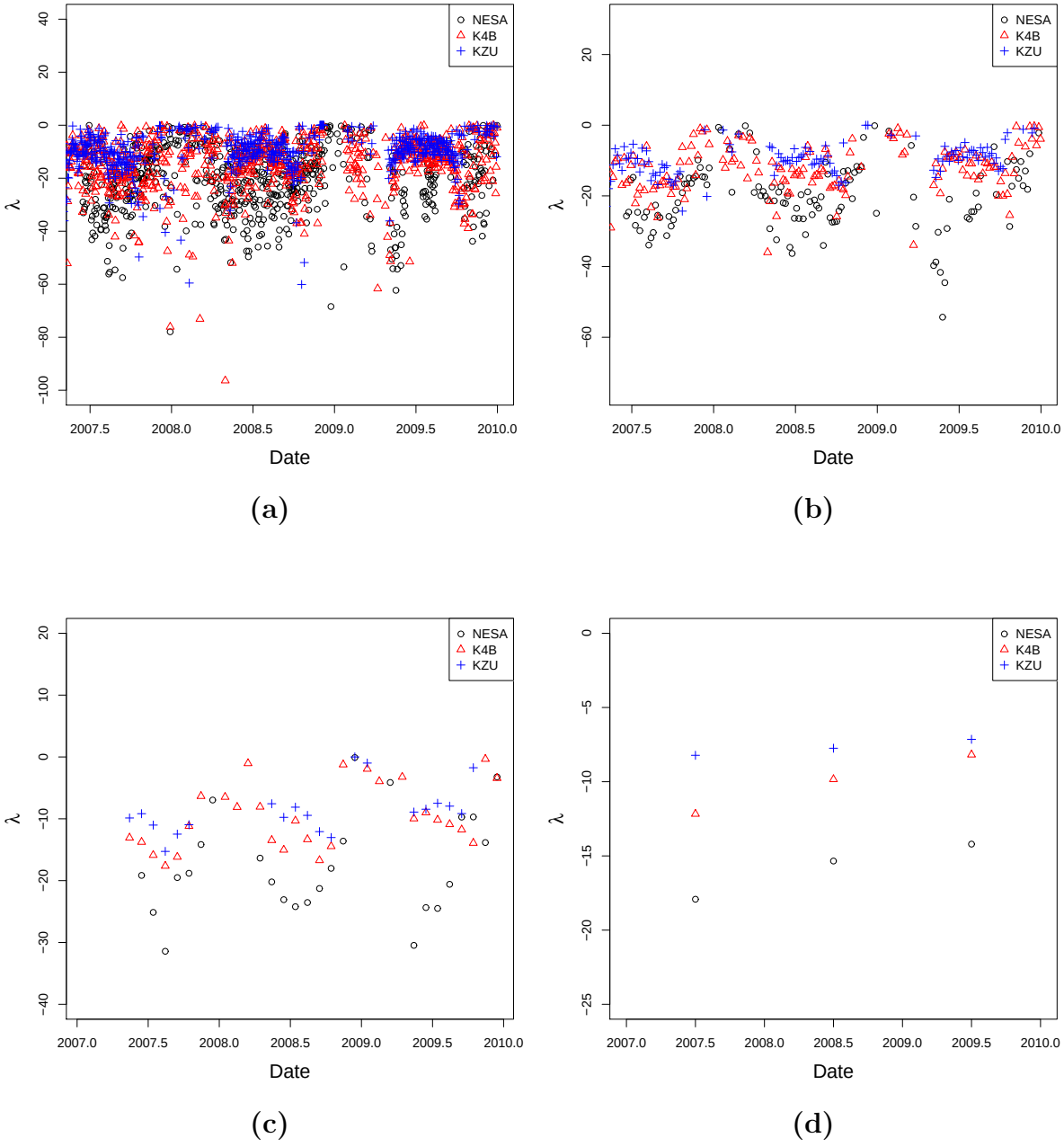

Figure 3.4 Comparison of the effect of timescale on water-use efficiency (λ) for all sites. Panel (a) daily averages, Panel (b) five-day averages, Panel (c) monthly averages, and Panel (d) annual averages for 2007-2009.

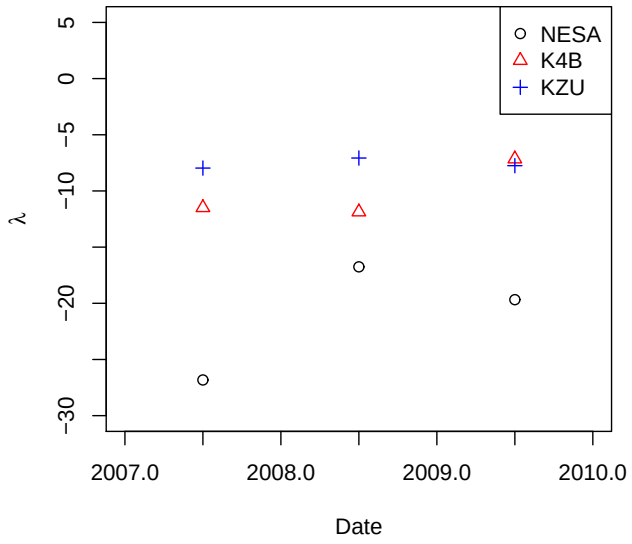

(a)

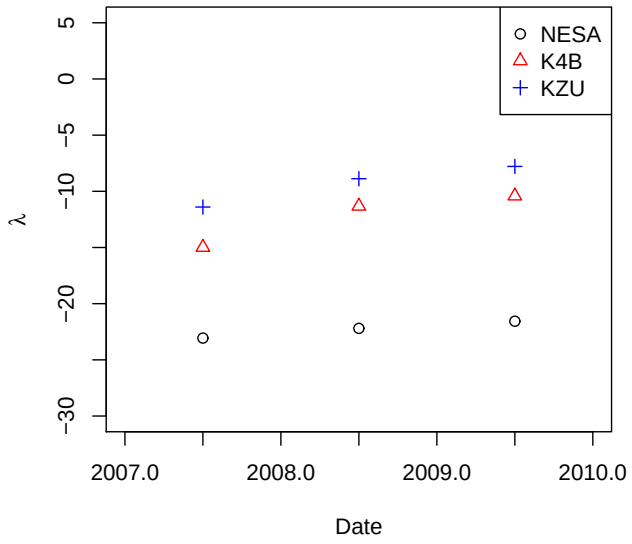

(b)

Figure 3.5 Comparison of the effect of seasonality on water-use efficiency (λ) for all sites. Panel (a) averages for spring season, Panel (b) averages for summer season for 2007-2009.

more in-depth in the Section 3.4.

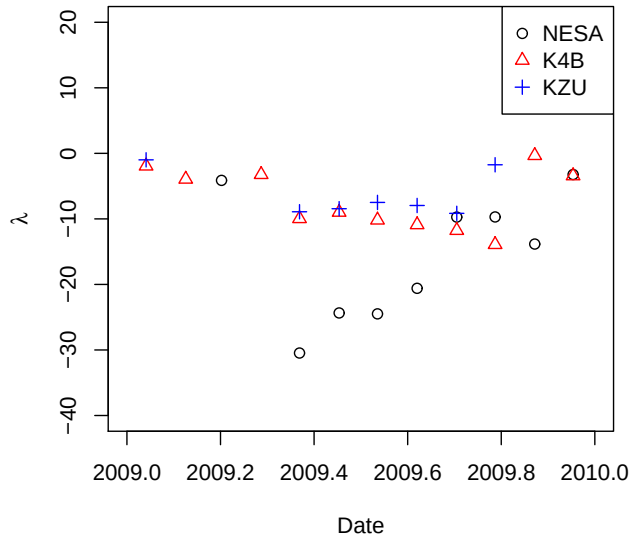

Figure 3.6 Mean monthly water-use efficiency(λ) for 2009 for each site.

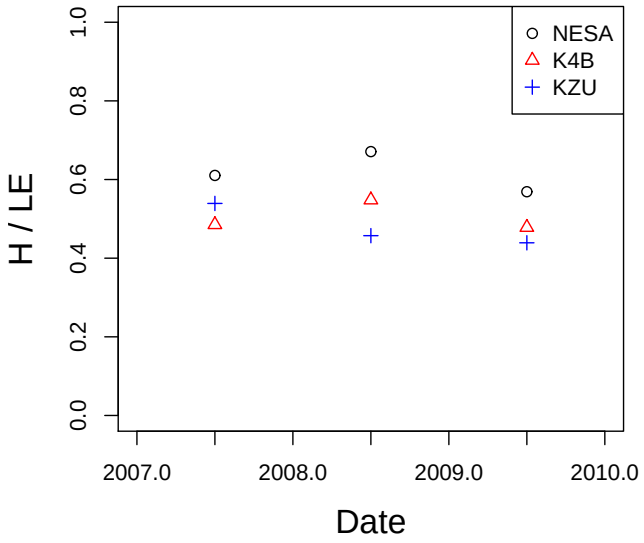

Figure 3.7 Mean annual Bowen ratio all for study sites during 2007-2009.

3.4 Discussion

3.4.1 Impact of Vegetation Composition

From the analysis it is apparent that water-use efficiency varies across sites. When examining λ values at different timescales (Figure 3.4), NESA generally has the most efficient values, followed by K4B, and finally KZU with the least efficient values. This does not seem to be a function of soil moisture, fetch distance or energy balance closure. As Figure 3.1 shows, this is not necessarily due to variability in net radiation from site to site, since peak values were relatively similar. Differences in partitioning of LE and H could possibly effect values of λ. However, after examining the mean annual Bowen ratio for each site, there is little variation across the years. Although KZU and K4B sites also exhibited higher LE and H values compared to NESA, this was most likely due to the greater amounts of precipitation and temperature at these sites.

The variability in λ across sites displays the influence of land cover and land use on λ. It appears that sites experiencing woody encroachment (NESA and K4B) show more efficient water-use than sites that are not experiencing woody encroachment (KZU). Similar results were found by Scott et al. (2006), where grasslands experiencing woody encroachment saw more efficient water-use than grasslands that were not. This was primarily due to the fact that the rooting depth of the woody-vegetation was much greater than grasses, which allowed woody vegetation to access deeper groundwater reserves. A recent study by Ratajczak et al. (2010) has confirmed this relationship at the K4B site. Grasses were found to access soil water down to 30 cm below the surface, while the rooting depth of shrubs were found to extend below 30 cm. Although KZU is comprised mostly of C_4 grasses, which Emmerich (2007) found to have more efficient water-use compared to C_3 plants, the rooting depth

of woody vegetation appears to be the factor contributing to higher water efficiencies. A similar relationship can be inferred at the NESA site, where rooting depth of woody-vegetation exceeds that of grasses, and results in more efficient λ values.

3.4.2 Impact of Seasonality

Different trends in λ can also be seen at different time scales. Evaluating mean seasonal (Figure 3.5) and annual values (Figure 3.4) for KZU, there is little or no variability during the spring months and a slight decrease in efficiency during the summer months and mean annual values. K4B and NESA sites typically saw a general decrease in efficiency for summer and inter-annual scales. Between the 2007 and 2008 spring λ values, K4B experienced similar values of efficiency while NESA experienced a sharp decrease in efficiency. However, in 2009 K4B saw a sharp decrease in efficiency, while NESA showed an increase in efficiency. This phenomena was shown in the monthly averages of λ for 2009 in Figure 3.6. After the burn, NESA exhibits much more efficient water-use than the other sites, while K4B exhibited much less efficient values of water-use compared to previous years. Possible explanations for this is that unlike K4B, any woody-vegetation left after burns at NESA are physically removed from the site, whereas K4B has experienced woody encroachment for a much longer time and remaining woody-vegetation was not removed. Unlike the K4B site, the removal of the remaining unburned biomass at NESA allows for a greater opportunity for new vegetation to grow in its place. Hence, more carbon would be assimilated at NESA and therefore would show greater water-use efficiencies.

Examining seasonal and inter-annual variability in λ across the sites, land cover and land use is important. Unlike the two other sites, annual prescribed burns at KZU inhibit woody encroachment. Therefore, KZU shows the most homogeneity of any of the sites and the most consistent composition through time. This is interesting when

compared to the K4B site, which experiences virtually the same energy balance partitioning and precipitation amounts due to its close proximity to KZU. However, K4B generally experiences more efficient values of water use than KZU. This discrepancy in λ between these two sites is most likely due to variation in surface homogeneity and vegetation across the sites. Greater variation in vegetation composition leads to more diversity in plant species, each with different growing seasons and adaptations that may make them more suitable for local conditions. This may be a possible explanation to why variability in water-use efficiency is seen between sites that are experiencing woody-encroachment and those that are not. Since K4B is experiencing woody encroachment, variability in λ is most likely due to variation in vegetation composition, whereas KZU is more dependent on variation in precipitation. This may also explain why there was little variation in λ values at KZU, due to the similar values of annual precipitation received at this site. Since NESA also experienced woody encroachment, vegetation composition was the most likely factor in contributing variability into λ. In addition, more efficient values of λ were likely due to the lower average annual temperature NESA experienced compared to the other sites.

3.5 Conclusions

Water-use efficiency was compared to three different grassland ecosystems. It was found that grasslands in this study not experiencing woody-encroachment and are more homogeneous generally show less-efficient water-use than grasslands experiencing woody-encroachment. A possible explanation for this may be due to the fact that woody plants typically have deeper rooting depths than grasses and are able to access deeper ground water reserves. This means that these plants are less susceptible to water stress and have greater water-use efficiency. Therefore, sites experiencing

woody-encroachment typically experienced more efficient water use. Site-specific variations in λ were more readily observed at seasonal and inter-annual timescales rather than daily and monthly averages.

Implications of climate and land cover/use change have significant consequences on grassland ecosystems and how they function. Increasing temperatures and variability in precipitation intensity and frequency could alter the efficiency with which plants assimilate carbon. Climate change may also create more optimal conditions for different plant species. Changes in land management can also have profound effects on grassland ecosystem function. As suggested in this study, human activities such as fire suppression and land-use changes have altered how grassland ecosystems assimilate carbon.

Chapter 4

Conclusion

In this study, the eddy covariance technique was used to analyze how variations in land cover impact grasslands. In Chapter 2, an overview of the eddy covariance method and data processing procedures was presented. The underlying theory of the eddy-covariance technique was presented, along with the governing equations. Processing procedures, such as spike/lag removal, signal corrections, coordinate rotation, Webb-Pearman-Leuning corrections, and quality control methods were discussed. Issues with spatial heterogeneity and long-term measurements were outlined as well.

In Chapter 3 the impact of land-cover change on water-use efficiency in grasslands was examined. Here, three grassland ecosystems were studied, one grassland that experienced annual burning with a relatively homogeneous vegetation composition, while the remaining two grasslands experienced woody encroachment and prescribed burns every four years. It was concluded that variation in water-use efficiency between the three grasslands was due to vegetation composition.

There are several possible methods to more accurately quantify the conclusions in Chapter 3. A full ecological profile of the study areas could be conducted to better understand the vegetation composition of the study areas. Several possible methods

could be used, including remote sensing and atmospheric sampling of oxygen isotopes. High-resolution remote sensing imagery could be used to assess the Normalized Difference Vegetation Index (NDVI) within the tower footprint. This could help differentiate vegetation within the footprint area, and give insight to samples from various contribution areas. Atmospheric sampling can also be used to determine C_3 and C_4 plant species composition using oxygen isotopes.

In regard to improving the eddy covariance technique, it is the author's recommendation that there needs to be a greater effort in the study of the eddy covariance method and the temporal scales used in the averaging of fluxes. It is the author's belief that some of the issues with the eddy covariance system, specifically the energy balance closure problem, lie within the spatial and temporal averaging of turbulent fluxes. Studies by Huang et al. (2009) and Foken et al. (2009) have shown that surface heterogeneity can cause secondary circulations and other turbulent motions that do not interact with the surface, and therefore cannot be measured by the eddy covariance system. Since secondary circulations transport energy and are unable to be measured at the surface, the energy budget cannot be closed at the small scale with this methodology Foken et al. (2009). Another suggestion is that a standardized methodology in sampling correction should also be implemented. This may provide a much easier pathway to debug and correct possible issues.

From this study, the eddy covariance technique has proven to be a useful tool to study the exchange of energy and mass between the surface and the atmosphere. At the current time, it is the premier method to conduct these measurements. Although it has been proven to be a useful method, it has its pitfalls. To this end, the energy balance closure problem appears to be the greatest weakness of the system. It is important that research continues to correct these issues. Resolving these problems will not only strengthen the value of the eddy covariance technique, but as a whole help

the scientific community better understand interactions within earth's ecosystems.

Bibliography

Anderson, D. E., S. B. Verma, and N. J. Rosenberg, 1984: Eddy correlation measurements of CO2 , latent heat, and sensible heat fluxes over a crop surface. *Boundary-Layer Meteorology*, **29 (3)**, 263–272.

Archer, S., T. W. Boutton, and K. A. Hibbard, 2001: *Trees in Grasslands: Biogeochemical Consequences of Woody Plant Expansion*, 115–138. Academic Press, San Diego, CA.

Aubinet, M., 2008: Eddy covariance CO2 flux measurements in nocturnal conditions: an analysis of the problem. *Ecological Applications*, **18 (6)**, 1368–1378.

Aubinet, M., et al., 2000: Estimates of the annual net carbon and water exchange of forests: the EUROFLUX methodology. *Advances in Ecological Research*, **30**, 113–175, doi:10.1016/S0065-2504(08)60018-5.

Baldocchi, D., 1994: A comparative study of mass and energy exchange rates over a closed C3 (wheat) and an open C4 (corn) crop: II. CO2 exchange and water use efficiency. *Agricultural and Forest Meteorology*, **67 (3-4)**, 291–321, doi:10.1016/0168-1923(94)90008-6.

Baldocchi, D., 2003: Assessing the eddy covariance technique for evaluating carbon

dioxide exchange rates of ecosystems: past, present and future. *Global Change Biology*, **9 (4)**, 479–492, doi:10.1046/j.1365-2486.2003.00629.x.

Baldocchi, D., et al., 2001a: FLUXNET: a new tool to study the temporal and spatial variability of ecosystem-scale carbon dioxide, water vapor, and energy flux densities. *Bulletin of the American Meteorological Society*, **82 (11)**, 2415–2434.

Baldocchi, D., et al., 2001b: FLUXNET: a new tool to study the temporal and spatial variability of ecosystem-scale carbon dioxide, water vapor, and energy flux densities. *Bulletin of the American Meteorological Society*, **82 (11)**, 2415–2434.

Baum, K., J. Ham, N. Brunsell, and P. Coyne, 2008: Surface boundary layer of cattle feedlots: Implications for air emissions measurement. *Agricultural and Forest Meteorology*, **148 (11)**, 1882–1893, doi:10.1016/j.agrformet.2008.06.017.

Beer, C., et al., 2009: Temporal and among-site variability of inherent water use efficiency at the ecosystem level. *Global Biogeochemical Cycles*, **23 (2)**, doi:10.1029/2008GB003233.

Billings, S. A., 2006: Soil organic matter dynamics and land use change at a grassland/forest ecotone. *Soil Biology and Biochemistry*, **38 (9)**, 2934–2943, doi:10.1016/j.soilbio.2006.05.004.

Briggs, J., A. Knapp, J. Blair, J. Heisler, G. Hoch, M. Lett, and J. McCarron, 2005: An ecosystem in transition: causes and consequences of the conversion of mesic grassland to shrubland. *BioScience*, **55 (3)**, 243–254, doi:10.1641/0006-3568(2005)055[0243:AEITCA]2.0.CO;2.

Brunsell, N. A., T. L. Buck, J. M. Ham, S. Billings, and J. Nippert, 2010a: Surface-atmosphere coupling of carbon and water fluxes in a mixed grassland. *Theoretical and Applied Climatology*, in review.

Brunsell, N. A., A. R. Jones, T. L. Jackson, and J. J. Feddema, 2010b: Seasonal trends in air temperature and precipitation in IPCC AR4 GCM output for Kansas, USA: evaluation and implications. *International Journal of Climatology*, in press, doi:10.1002/joc.1958.

Buckley, T., J. Miller, and G. Farquhar, 2002: The mathematics of linked optimisation for water and nitrogen use in a canopy. *Silva Fennica*, **36 (3)**, 639–669.

Burke, I., T. Kittel, W. Lauenroth, P. Snook, C. Yonker, and W. Parton, 1991: Regional analysis of the central Great Plains. *BioScience*, **41 (10)**, 685–692.

Burkinshaw, A. M. and E. W. Bork, 2009: Shrub encroachment impacts the potential for multiple use conflicts on public land. *Environmental Management*, **44 (3)**, 493–504, doi:10.1007/s00267-009-9328-2.

Clement, R., 1999: EdiRe. University of Edinburgh, Edinbrugh, UK.

Collins, S., 1992: Fire frequency and community heterogeneity in tallgrass prairie vegetation. *Ecology*, **73 (6)**, 2001–2006.

Cowan, I. R. and G. D. Farquhar, 1977: *Stomatal function in relation to leaf metabolism and environment*, 471– 505. Cambridge Univ. Press, Cambridge, U.K.

Dale, V. H., 1997: the Relationship Between Land-Use Change and Climate Change. *Ecological Applications*, **7 (3)**, 753–769.

Eggemeyer, K. and S. Schwinning, 2009: Biogeography of woody encroachment: why is mesquite excluded from shallow soils? *Ecohydrology*, **2 (1)**, 81–87.

Emmerich, W., 2007: Ecosystem water use efficiency in a semiarid shrubland and grassland community. *Rangeland Ecology & Management*, **60 (5)**, 464–470.

Falge, E., et al., 2001: Gap filling strategies for long term energy flux data sets. *Agricultural and Forest Meteorology*, **107 (1)**, 71–77, doi:DOI:10.1016/S0168-1923(00)00235-5.

Falge, E., et al., 2002: Seasonality of ecosystem respiration and gross primary production as derived from FLUXNET measurements. *Agricultural and Forest Meteorology*, **113 (1-4)**, 53–74.

FAO, 2009: Grasslands: enabling their potential to contribute to greenhouse gas mitigation. 1–5 pp.

Finnigan, J., 2004: A re-evaluation of long-term flux measurement techniques Part II: coordinate systems. *Boundary-layer meteorology*, **113 (1)**, 1–41.

Finnigan, J., R. Clement, Y. Malhi, R. Leuning, and H. Cleugh, 2003: A re-evaluation of long-term flux measurement techniques part I: averaging and coordinate rotation. *Boundary-Layer Meteorology*, **107 (1)**, 1–48.

Fitch, H. and W. Kettle, 1988: Kansas ecological reserves (University of Kansas natural areas). *Transactions of the Kansas Academy of Science*, **91 (1)**, 30–36, doi:10.2307/3628292.

Flanagan, L. B., L. a. Wever, and P. J. Carlson, 2002: Seasonal and interannual variation in carbon dioxide exchange and carbon balance in a northern temperate grassland. *Global Change Biology*, **8 (7)**, 599–615, doi:10.1046/j.1365-2486.2002.00491.x.

Foken, T., M. G, M. Mauder, L. Mahrt, B. Amiro, and W. Munger, 2004: *Post-field data quality control*, chap. Handbook o, 181–208. 1988, Kluwer Academic Publishers.

Foken, T. and B. Wichura, 1996: Tools for quality assessment of surface-based flux measurements. *Agricultural and Forest Meteorology*, **78 (1-2)**, 83–105.

Foken, T., F. Wimmer, M. Mauder, C. Thomas, and C. Liebethal, 2006: Some aspects of the energy balance closure problem. *Atmospheric Chemistry and Physics*, **6**, 4395–4402.

Foken, T., et al., 2009: Energy balance closure for the LITFASS-2003 experiment. *Theoretical and Applied Climatology*, doi:10.1007/s00704-009-0216-8.

Fuehrer, P. and C. Friehe, 2002: Flux corrections revisited. *Boundary-Layer Meteorology*, **102 (3)**, 415–458, doi:10.1175/1520-0469(1977)034⟨0515:FMFETA⟩2.0.CO;2.

Goulden, M. L., 1996: Carbon assimilation and water-use efficiency by neighboring Mediterranean-climate oaks that differ in water access. *Tree Physiology*, **16 (4)**, 417–24.

Hall, D. O., D. S. Ojima, W. J. Parton, and J. M. O. Scurlock, 1995: Response of temperate and tropical grasslands to CO2 and climate change. *Journal of Biogeography*, **22 (2)**, 537–547.

Ham, J. and J. Heilman, 2003: Experimental test of density and energy-balance corrections on carbon dioxide flux as measured using open-path eddy covariance. *Agronomy Journal*, **95 (6)**, 1393.

Hammerle, A., A. Haslwanter, M. Schmitt, M. Bahn, U. Tappeiner, A. Cernusca, and G. Wohlfahrt, 2007: Eddy covariance measurements of carbon dioxide, latent and sensible energy fluxes above a meadow on a mountain slope. *Boundary-Layer Meteorology*, **122 (2)**, 397–416, doi:10.1007/s10546-006-9109-x.

Haslwanter, A., A. Hammerle, and G. Wohlfahrt, 2009: Open-path vs. closed-path eddy covariance measurements of the net ecosystem carbon dioxide and water vapour exchange: A long-term perspective. *Agricultural and Forest*, **149 (2)**, 291–302, doi:10.1016/j.agrformet.2008.08.011.

Hayden, B., 1998: *Regional Climate and the Distribution of Tallgrass Prairie*, chap. Grassland, 19–34. Oxford University Press, New York, New York.

Højstrup, J., 1993: A statistical data screening procedure. *Measurement Science and Technology*, **4**, 153–157.

Hopkins, A. and A. Del Prado, 2007: Implications of climate change for grassland in Europe: impacts, adaptations and mitigation options: a review. *Grass and Forage Science*, **62 (2)**, 118–126, doi:10.1111/j.1365-2494.2007.00575.x.

Hsieh, C., G. Katul, and T. Chi, 2000: An approximate analytical model for footprint estimation of scalar fluxes in thermally stratified atmospheric flows. *Advances in Water Resources*, **23 (7)**, 765–772, doi:10.1016/S0309-1708(99)00042-1.

Huang, J., X. Lee, and E. G. Patton, 2009: Dissimilarity of Scalar Transport in the Convective Boundary Layer in Inhomogeneous Landscapes. *Boundary-Layer Meteorology*, **130 (3)**, 327–345, doi:10.1007/s10546-009-9356-8.

Huxman, T. E., et al., 2005: Ecohydrological implications of woody plant encroachment. *Ecology*, **86 (2)**, 308–319, doi:10.1890/03-0583.

Inagaki, A., M. O. Letzel, S. Raasch, and M. Kanda, 2006: Impact of surface heterogeneity on energy imbalance: A study using LES. *Journal of the Meteorological Society of Japan*, **84 (1)**, 187–198, doi:10.2151/jmsj.84.187.

Jackson, R., K. Farley, W. Hoffmann, E. Jobbágy, and R. McCulley, 2007: *Carbon and water tradeoffs in conversions to forests and shrublands*, chap. 19, 237–246. Springer, New York, New York.

Kaimal, J. C. and J. J. Finnigan, 1994: *Atmospheric Boundary Layer Flows: Their Structure and Movement*. Oxford University Press, New York, NY, 289 pp.

Knapp, A. K., et al., 2002: Rainfall variability, carbon cycling, and plant species diversity in a mesic grassland. *Science*, **298 (5601)**, 2202–2205, doi:10.1126/science.1076347.

Kuglitsch, F. G., et al., 2008: Characterisation of ecosystem water-use efficiency of european forests from eddy covariance measurements. *Biogeosciences Discussions*, **5 (6)**, 4481–4519, doi:10.5194/bgd-5-4481-2008.

Law, B., et al., 2002: Environmental controls over carbon dioxide and water vapor exchange of terrestrial vegetation. *Agricultural and Forest Meteorology*, **113 (1-4)**, 97–120.

Lee, X., W. Massman, and B. Law, 2004: *Handbook of Micrometerology: A Guide For Surface Flux Measurement and Analysis*. Kluwer Academic Publishers, Dordrecht, The Netherlands, 250 pp.

Leuning, R., 2007: The correct form of the Webb, Pearman and Leuning equation for eddy fluxes of trace gases in steady and non-steady state, horizontally homogeneous flows. *Boundary-Layer Meteorology*, **123 (2)**, 263–267.

Lloyd, J. and J. Taylor, 1994: On the temperature dependence of soil respiration. *Functional Ecology*, **8 (3)**, 315–323.

Massman, W., 2000: A simple method for estimating frequency response corrections for eddy covariance systems. *Agricultural and Forest Meteorology*, **104 (3)**, 185–198, doi:10.1016/S0168-1923(00)00164-7.

Massman, W. and X. Lee, 2002: Eddy covariance flux corrections and uncertainties in long-term studies of carbon and energy exchanges. *Agricultural and Forest Meteorology*, **113 (1-4)**, 121–144, doi:10.1016/S0168-1923(02)00105-3.

Mauder, M., T. Foken, R. Clement, J. A. Elbers, W. Eugster, T. Grünwald, B. Heusinkveld, and O. Kolle, 2008: Quality control of CarboEurope flux data Part 2: Inter-comparison of eddy-covariance software. *Biogeosciences*, **5 (2)**, 451–462, doi:10.5194/bg-5-451-2008.

McKinley, D. and J. Blair, 2008: Woody plant encroachment by Juniperus virginiana in a mesic native grassland promotes rapid carbon and nitrogen accrual. *Ecosystems*, **11 (3)**, 454–468, doi:10.1007/s10021-008-9133-4.

McMillen, R. T., 1988: An eddy correlation technique with extended applicability to non-simple terrain. *Boundary-Layer Meteorology*, **43 (3)**, 231–245, doi:10.1007/BF00128405.

Moffat, A., et al., 2007: Comprehensive comparison of gap-filling techniques for eddy covariance net carbon fluxes. *Agricultural and Forest Meteorology*, **147 (3-4)**, 209–232, doi:10.1016/j.agrformet.2007.08.011.

Monson, R., M. Sackschewsky, and G. Williams, 1986: Field measurements of photosynthesis, water-use efficiency, and growth in Agropyron smithii (C$_{3}$) and Bouteloua gracilis (C $_{4}$) in the Colorado shortgrass steppe. Springer, 400–409 pp.

Moore, C., 1986: Frequency response corrections for eddy correlation systems. *Boundary-Layer Meteorology*, **37**, 12–35.

Nippert, J. B., P. a. Fay, J. D. Carlisle, A. K. Knapp, and M. D. Smith, 2009: Ecophysiological responses of two dominant grasses to altered temperature and precipitation regimes. *Acta Oecologica*, **35 (3)**, 400–408, doi:10.1016/j.actao.2009.01.010.

Nippert, J. B. and A. K. Knapp, 2007: Linking water uptake with rooting patterns in grassland species. *Oecologia*, **153 (2)**, 261–72, doi:10.1007/s00442-007-0745-8.

Novick, K. A., P. C. Stoy, G. G. Katul, D. S. Ellsworth, M. B. S. Siqueira, J. Juang, and R. Oren, 2004: Carbon dioxide and water vapor exchange in a warm temperate grassland. *Oecologia*, **138 (2)**, 259–74, doi:10.1007/s00442-003-1388-z.

Ojima, D. S., B. O. M. Dirks, E. P. Glenn, C. E. Owensby, and J. O. Scurlock, 1993: Assessment of C budget for grasslands and drylands of the world. *Water, Air, and Soil Pollution*, **70**, 95–109.

Panin, G. N., G. Tetzlaff, and a. Raabe, 1998: Inhomogeneity of the Land Surface and Problems in theParameterization of Surface Fluxes in Natural Conditions. *Theoretical and Applied Climatology*, **60 (1-4)**, 163–178, doi:10.1007/s007040050041.

Paw U, K., D. Baldocchi, T. Meyers, and K. Wilson, 2000: Correction of eddy-covariance measurements incorporating both advective effects and density fluxes. *Boundary-Layer Meteorology*, **97 (3)**, 487–511.

Ponton, S., L. Flanagan, K. Alstad, B. Johnson, K. Morgenstern, N. Kljun, T. Black, and A. Barr, 2006: Comparison of ecosystem water-use efficiency among Douglas-fir forest, aspen forest and grassland using eddy covariance and carbon isotope

techniques. *Global Change Biology*, **12 (2)**, 294–310, doi:10.1111/j.1365-2486.2005.01103.x.

Ratajczak, Z., J. B. Nippert, J. C. Hartman, and T. Ocheltree, 2010: Positive feedbacks mechanisms drive shrub encroachment in tallgrass prairie. *Oecologia*, in review.

Schmid, H., 2002: Footprint modeling for vegetation atmosphere exchange studies: a review and perspective. *Agricultural and Forest Meteorology*, **113 (1-4)**, 159–183.

Schmid, H. and C. Lloyd, 1998: Spatial representativeness and the location bias of flux footprints over inhomogeneous areas. *Agricultural and Forest Meteorology*, **93 (3)**, 195.

Schotanus, P., F. Nieuwstadt, and H. Bruin, 1983: Temperature measurement with a sonic anemometer and its application to heat and moisture fluxes. *Boundary-Layer Meteorology*, **26 (1)**, 81–93.

Scott, R. L., T. E. Huxman, D. G. Williams, and D. C. Goodrich, 2006: Ecohydrological impacts of woody-plant encroachment: seasonal patterns of water and carbon dioxide exchange within a semiarid riparian environment. *Global Change Biology*, **12 (2)**, 311–324, doi:10.1111/j.1365-2486.2005.01093.x.

Scurlock, J. and D. Hall, 1998: The global carbon sink: a grassland perspective. *Global Change Biology*, **4 (2)**, 229–233, doi:10.1046/j.1365-2486.1998.00151.x.

Soussana, J.-F. and a. Lüscher, 2007: Temperate grasslands and global atmospheric change: a review. *Grass and Forage Science*, **62 (2)**, 127–134, doi:10.1111/j.1365-2494.2007.00577.x.

Stull, R., 1988: *An Introduction to Boundary Layer Meteorology*. Kluwer Academic Publishers, Dordrecht, The Netherlands, 670 pp.

The MathWorks, I., 2008: MATLAB. The MathWorks, Inc., Natick, Maryland.

Thornley, J. and M. Cannell, 1997: Temperate grassland responses to climate change: an analysis using the Hurley pasture model. *Annals of Botany*, **80 (2)**, 205, doi: 10.1006/anbo.1997.0430.

Twine, T., et al., 2000: Correcting eddy-covariance flux underestimates over a grassland. *Agricultural and Forest Meteorology*, **103 (3)**, 279–300, doi:10.1016/S0168-1923(00)00123-4.

Vickers, D. and L. Mahrt, 1997: Quality control and flux sampling problems for tower and aircraft data. *Journal of Atmospheric and Oceanic Technology*, **14 (3)**, 512–526, doi:10.1175/1520-0426(1997)014⟨0512:QCAFSP⟩2.0.CO;2.

Vitousek, P., H. Mooney, J. Lubchenco, and J. Melillo, 1997: Human domination of Earths ecosystems. *Urban Ecology*, **278 (5335)**, 3–13.

Webb, E., G. Pearman, and R. Leuning, 1980: Correction of flux measurements for density effects due to heat and water vapour transfer. *Quarterly Journal of the Royal Meteorological Society*, **106 (447)**, 85–100.

Wilczak, J., S. Oncley, and S. Stage, 2001: Sonic anemometer tilt correction algorithms. *Boundary-Layer Meteorology*, **99 (1)**, 127–150.

Wilson, K., et al., 2002: Energy balance closure at FLUXNET sites. *Agricultural and Forest Meteorology*, **113 (1-4)**, 223–243.

Xu, L. and D. D. Baldocchi, 2004: Seasonal variation in carbon dioxide exchange over a Mediterranean annual grassland in California. *Agricultural and Forest Meteorology*, **123 (1-2)**, 79–96, doi:10.1016/j.agrformet.2003.10.004.